Statistical Parametric Mapping of ^{99m}Tc-ECD SPECT in Idiopathic Parkinson's Disease and Multiple System Atrophy with Predominant Parkinsonian Features: Correlation with Clinical Parameters

Koen Van Laere, MD, PhD, DrSc[1]; Patrick Santens, MD, PhD[2]; Tommy Bosman, MD[2]; Jacques De Reuck, MD, PhD[2]; Luc Mortelmans, MD, PhD[1]; and Rudi Dierckx, MD, PhD[3]

[1]Division of Nuclear Medicine, Leuven University Hospital, Leuven, Belgium; [2]Department of Neurology, Ghent University Hospital, Ghent, Belgium; and [3]Division of Nuclear Medicine, Ghent University Hospital, Ghent, Belgium

Statistical parametric mapping was performed to investigate differences in regional cerebral blood flow (rCBF) between patients with idiopathic Parkinson's disease (IPD), patients with multiple system atrophy (MSA), and healthy volunteers. In addition, a voxel-based covariance analysis was performed with disease-specific parameters and clinical patient data such as disease duration, medication, and clinical subscores. **Methods:** For this purpose, ^{99m}Tc-ethylcysteine dimer (ECD) SPECT was performed on 81 IPD patients (50 men, 31 women; age, 62.6 ± 10.2 y), 15 MSA patients (9 men, 6 women; age, 61.5 ± 9.2 y), and 44 age- and sex-matched healthy volunteers (27 men, 17 women; age, 59.2 ± 11.9 y). **Results:** Significant hypoperfusion was observed in IPD compared with healthy subjects in a symmetric subcortical-cortical network including the basal ganglia, thalami, prefrontal and lateral frontal cortex, and parietooccipital cortex (voxel *P* value $P_{height} < 0.001$, corrected for multiple comparisons). For MSA, only symmetric hypoperfusion was seen in the putamen and thalamus with respect to healthy subjects and to IPD ($P_{height} < 0.01$, corrected). Prolonged disease duration or higher Hoehn and Yahr stage results in hypoperfusion of the posterior associative cortex. There is a negative correlation between perfusion of the caudate heads and limbic system and the standardized dosage of dopamine agonists in the patients with PD, whereas for MSA a bilateral decrease in putamen activity was noted ($P_{height} < 0.001$, uncorrected). Cognitive performance was positively correlated with limbic perfusion and inversely correlated with posterior associative cortical areas, but not with prefrontal regions. **Conclusion:** Voxel-based analysis of ^{99m}Tc-ECD perfusion SPECT shows detailed differences between IPD and MSA, which may be of use in the differentiation of both disease entities, and is able to elucidate cerebral perfusion correlates of disease severity, dopamine agonist medication, and cognitive performance.

Key Words: ^{99m}Tc-ECD SPECT; multiple system atrophy; Parkinson's disease; statistical parametric mapping; anatomic standardization

J Nucl Med 2004; 45:933–942

Idiopathic Parkinson's disease (IPD) and multiple system atrophy (MSA) are the 2 most common forms of parkinsonism, accounting for >90% of the cases. IPD accounts for 60%–85% and is characterized neuropathologically by a degeneration of brain stem nuclei, particularly the substantia nigra pars compacta, in association with the formation of neuronal Lewy bodies (*1*). This degeneration leads to functional alterations in basal ganglia synaptic activity, which is accompanied by alterations in regional cerebral glucose metabolism and blood flow. ^{18}F-FDG PET studies have described neuronal metabolic networks in IPD, which are characterized by lentiform and thalamic hypermetabolism at early stages, associated with regional metabolic decreases in the lateral frontal and paracentral cortical areas, corresponding to the lateral premotor cortex and the supplementary motor area (*2*). However, previous studies showed inconsistent results in the basal ganglia with reduced (*3*) or unchanged metabolic activity (*4*).

MSA includes striatonigral degeneration (SND or MSA-S), sporadic olivopontocerebellar atrophy, and Shy–Drager syndrome in its spectrum and is characterized clinically by a combination of extrapyramidal, pyramidal, autonomic, and cerebellar features. The pathology of MSA is distinct from that of IPD and is characterized by neuronal degeneration and gliosis in the nigrostriatal dopaminergic pathway,

Received Aug. 17, 2003; revision accepted Jan. 5, 2004.

For correspondence or reprints contact: Koen Van Laere, MD, PhD, DrSc, Nuclear Medicine Division, Leuven University Hospital, Herestraat 49, B-3000 Leuven, Belgium.

E-mail: koen.vanlaere@uz.kuleuven.ac.be

caudate and putamen, globus pallidus, brain stem, cerebellum, and spinal cord. About 10% of the patients thought to have PD during life are found to have MSA on autopsy (*5*). Previous ^{18}F-FDG PET studies in small groups of MSA patients have reported reduced levels of striatal, cerebellar, and brain stem glucose metabolism (*6–8*). Reduced lentiform nucleus glucose metabolism has also been reported in patients with clinically probable SND (*9*).

Separating parkinsonian syndromes using clinical criteria alone can be difficult but is important for treatment (pharmacologic, surgical, and experimental) and prognosis. In analogy to resting state studies of metabolism, resting state perfusion may be assessed as an indirect marker of neuronal function. Being more widely available than receptor tracers and ^{18}F-FDG PET, larger groups of patients can be studied using data-driven and observer-independent automated analysis. The possibility of performing automated volume-of-interest–based discriminant analysis to separate both IPD and MSA using perfusion SPECT has been shown (*10*). Voxel-based analysis enables a more detailed analysis with precise anatomic localization. Moreover, the effect of multiple covariates such as clinical parameters can be studied on a more precise regional level without a priori assumptions.

The aim of this study was to describe voxel-based cerebral perfusion correlates of IPD and MSA in comparison to healthy volunteers. Second, the neuronal correlates of clinical features in IPD and MSA were explored to identify the circuits involved in clinical alterations.

MATERIALS AND METHODS

Patients and Healthy Control Subjects

Eighty-one clinically probable, nondemented IPD patients (50 men, 31 women; age, 62.6 ± 10.2 y; disease duration, 11 ± 6.4 y) and 15 probable, nondemented MSA patients (9 men, 6 women; age, 61.5 ± 9.2 y; disease duration, 3.0 ± 2.2 y) were included in the study. The clinical diagnosis of IPD and MSA was accepted based on the Brain Bank criteria (*1*) and Quinn criteria (*5*), respectively. Full clinical data and follow-up information were available at the time of the SPECT, and the diagnosis was made before and independent of the SPECT scan results. The mean Hoehn and Yahr (H&Y) stage was 2.4 ± 1.1 y for both IPD and MSA. The dosage of levodopa analogs was expressed in milligrams, whereas dopamine agonist medication was expressed as the dosage equivalent of pergolide, using the equivalence ratio of 10 mg bromocriptine = 1 mg pergolide = 1 mg pramipexole = 4 mg ropinirole. Medication was at a stable level for at least 2 wk before the SPECT study. Based on Unified Parkinson Disease Rating Scale subscores and follow-up data, a severity index ranging from 1 to 4 was given (1 = absent, 2 = light, 3 = moderate, 4 = severe) for the following symptoms: tremor, bradykinesia, autonomic failure, and gait disturbance. Cognitive dysfunction was scored likewise, based on the presence of disturbances in daily functioning and neuropsychologic testing of memory attention, executive function, and visuospatial abilities (Mini-Mental State Examination, Dutch version of the Auditory Verbal Learning Test, controlled word association test, STROOP test, and Wisconsin Card Sorting test) (*11*). Results from complementary structural neuroimaging were available to support the clinical diagnostic criteria.

Forty-four healthy volunteers (27 men, 17 women; age, 59.2 ± 11.9 y) were selected at random from an available set of normal data to achieve age and sex matching. The recruitment, prescreening, and screening procedure as well as exclusion criteria for the healthy volunteers have been described previously (*12*).

The study was approved by the local ethics committee and all subjects gave written informed consent.

SPECT Data Acquisition and Reconstruction

^{99m}Tc-Ethylcysteine dimer (ECD) (Neurolite; Bristol-Myers-Squibb/Dupont Pharmaceuticals) was used. All subjects were scanned under standard circumstances: dimly lit room, eyes closed, and minimal background noise. Data were acquired with patients in the "ON" state and scanning was initiated 30 min after injection. The first 62 patient SPECT images were acquired by means of a dual-head Helix system (Elscint/General Electric), whereas the most recent 34 scans were acquired on a triple-head γ-camera (Toshiba GCA-9300A; Dutoit Medical), equipped with parallel-hole, low-energy, high-resolution collimators. For the former scans, acquisition was done over 20 min, 60 angles through 360° in step-and-shoot mode. The triple-head data were acquired over 90 angles through 360° in continuous mode over 20 min and data were rebinned in 4° parallel bins. All acquisitions were done in a 128 × 128 matrix. Reconstruction was done using filtered backprojection (HERMES; Nuclear Diagnostic) with a Butterworth filter (order, 8; cutoff, 0.40 cm^{-1}). Uniform Sorenson attenuation correction was used with an attenuation coefficient of 0.09 cm^{-1} (*13*). Triple-head data were corrected to the lower-resolution parallel dual-head data using our previously validated transfer procedure based on isotropic resolution correction (*13*). Data of the healthy volunteers were acquired on the Helix system. Possible remaining camera acquisition effects were considered by using the camera type as a nuisance variable in the subsequent statistical analysis.

Image Transformations and Data Analysis

Images were analyzed using statistical parametric mapping (SPM99; Wellcome Department of Cognitive Neurology, Institute of Neurology, London, U.K.; http://www.fil.ion.ucl.ac.uk/spm/). All SPM calculations were performed using Matlab version 6.5 (The MathWorks Inc.). Anatomic standardization was performed by a nonlinear transformation using 3 × 4 × 3 basis functions and 5 nonlinear iterations to the generic SPM99 SPECT template. A resulting voxel size of 3 × 3 × 3 mm was used. The normalized studies were smoothed with an isotropic 14-mm kernel.

A single-subject design was used (disease groups were modeled as different conditions) with covariates of interest or nuisance variables. Covariates were centered around the "condition" mean and correlated within condition (i.e., patient group). Unless stated otherwise, regions were reported as significant if they contained voxels with a value of at least $P_{height} < 0.05$, corrected for multiple comparisons, with cluster extent threshold (k_E) = 20 (corresponding to 0.5 mL). Where explicitly indicated, uncorrected values of at least $P_{height} < 0.01$ are also reported, for those regions where a priori information is available (e.g., known motor circuit connections) or where explicit hypotheses were considered (e.g., effect of medication in the striatum).

Covariance analysis was performed to extract regions whose changes in regional cerebral blood flow (rCBF) correlated significantly with changes in disease variables or clinical scores. The sex

and camera type were used as nuisance variables. The mean global activity of each scan was adjusted to a grand mean of 50 mL/100 mL/min using a proportional scaling scheme. The analysis threshold for gray matter was put at 0.80.

Talairach brain coordinates were given by a nonlinear transform to Talairach space (*14*) (http://www.mrc-cbu.cam.ac.uk/Imaging/mnispace.html); these are given in the tables. Talairach Daemon software was used for conversion into Brodmann localization (http://ric.uthscsa.edu/projects/talairachdaemon.html).

All images for patients with predominantly right-handed symptoms were flipped left to right to represent a more uniform population sample. Group analyses were performed with and without flipping of the right-sided symptom IPD patients.

Since the clinical variables disease duration, H&Y score, and overall symptom severity are highly correlated, we chose to collapse these covariates into one as a measure of disease progression. To describe the differences with healthy subjects for patients with relatively short disease duration, a classification design was also used with separation into a subgroup with disease duration between 0 and 5 y ($n = 20$; average duration, 3.1 ± 1.7 y) and a group with long disease duration ($n = 61$; 5–20 y; average duration, 12.9 ± 3.8 y).

Conventional statistics between clinical scores for the different subject groups were performed using SPSS version 11.0 (SPSS Inc.).

RESULTS

Clinical Variables

Demographic and clinical data are given in Table 1 for both patient groups. The study groups were comparable for disease severity expressed as H&Y score, both in the on and off situation. There was a highly significant correlation between H&Y stage and disease duration in the IPD group (Pearson $\rho = 0.328$, $P = 0.003$ for the ON condition; $\rho = 0.449$, $P < 0.001$ for the OFF condition). As expected from its more rapid clinical course, MSA patients had a lower average disease duration: 3.0 y versus 11.0 y ($P < 0.001$).

There was also a significant difference in clinical motor symptom lateralization between IPD and MSA ($P < 0.001$): for MSA, only 4 of 15 patients showed lateralized symptoms (all to the left), whereas 68 of 81 IPD patients showed clinical lateralization (30 right, 38 left). The dosage of medication used was not different between both patient groups, both for levodopa and for dopamine agonists. MSA patients used more additional drugs ($P = 0.02$). Of the clinical symptom parameters, autonomic failure ($P < 0.001$) and speech dysfunction ($P = 0.008$) were more prominent in the MSA group compared with the IPD group.

Regional Perfusion: Group Differences

Both patient groups and healthy subjects showed similar age-dependent perfusion patterns with decreased anterior cingulate, medial frontal, left and right frontotemporal, and caudate head decreases with increasing age. From a multiregression design, there were no clusters with a significant difference between the healthy subjects and patient groups regarding the age dependence of rCBF in the age range considered.

TABLE 1
Patient Characteristics and Semiquantitative Symptom Scores

Parameter	Group	
	IPD ($n = 81$)	MSA ($n = 15$)
Age (y)	62.6 ± 10.2	61.4 ± 9.2
Gender (M/F)	50/31	9/6
Symptom duration (y)	11.0 ± 6.4	3.0 ± 2.2
H&Y score ON	2.4 ± 1.1	2.4 ± 1.1
H&Y score OFF	2.8 ± 1.2	2.4 ± 1.1
Lateralization (L/none/R)	38/13/30	4/11/0
Levodopa medication* (mg)	690 ± 410	430 ± 460
D_2-agonist medication† (mg)	3.12 ± 4.13	1.75 ± 2.14
Other drugs (*n*)	43/81	3/15
Semiquantitative symptom score		
Gait disturbances	2.77 ± 0.87	2.77 ± 0.73
Tremor	2.33 ± 1.11	1.60 ± 0.91
Starting blockade	2.20 ± 1.20	1.55 ± 0.93
Akinesia	2.51 ± 0.94	2.27 ± 0.88
Cognitive performance	1.49 ± 0.83	1.47 ± 0.74
Ophthalmologic score	1.26 ± 0.56	1.60 ± 0.83
Speech and swallow	1.83 ± 0.89	2.67 ± 0.98
Autonomous symptoms	1.15 ± 0.47	2.40 ± 1.07
Postural stability	1.44 ± 0.93	1.92 ± 1.26

*Expressed as equivalent levodopa dose (mg).
†Expressed as equivalent bromocriptine dose (mg).
Data are expressed as mean ± SD unless indicated otherwise.

IPD Versus Healthy Subjects. Significant hypoperfusion in IPD was present compared with healthy subjects in a symmetric subcortical circuit ranging from the substantia nigra, bilateral thalami, and lentiform nuclei. There was also involvement of the (mainly right) prefrontal cortex and lateral frontal cortex (supplementary motor region) (Brodmann area [BA] 8, 9, and 10), as well as the right middle temporal gyrus (BA 21), right and left bilateral parietal association cortex, including the precuneus (BA 7, 40) and bilateral occipital cortex ($P < 0.001$, corrected) (Fig. 1A).

The contrast of relative hyperperfusion for IPD versus healthy subjects showed significant clusters in the vermis and bilateral (mainly right) upper cerebellar hemisphere at $P_{height} < 0.001$ (uncorrected). These results are also included in Figure 1. Probabilistic locations and the significance of the clusters are given for both contrasts in Table 2.

MSA Versus Healthy Subjects. In the case of MSA versus healthy subjects, a symmetric hypoperfusion was found in the lentiform nucleus, especially in the dorsal putamen, anterior mesencephalon (ventral lateral thalamus) ($P < 0.001$, corrected). A smaller cluster in the right middle frontal gyrus (mainly BA 6, 8) was found, but no significant prefrontal or parietal involvement was present.

The results are shown in Figure 1B; cluster locations with significance levels are given in Table 2.

IPD Versus MSA. When comparing IPD and MSA directly, relative hypoperfusion of the bilateral posterior pu-

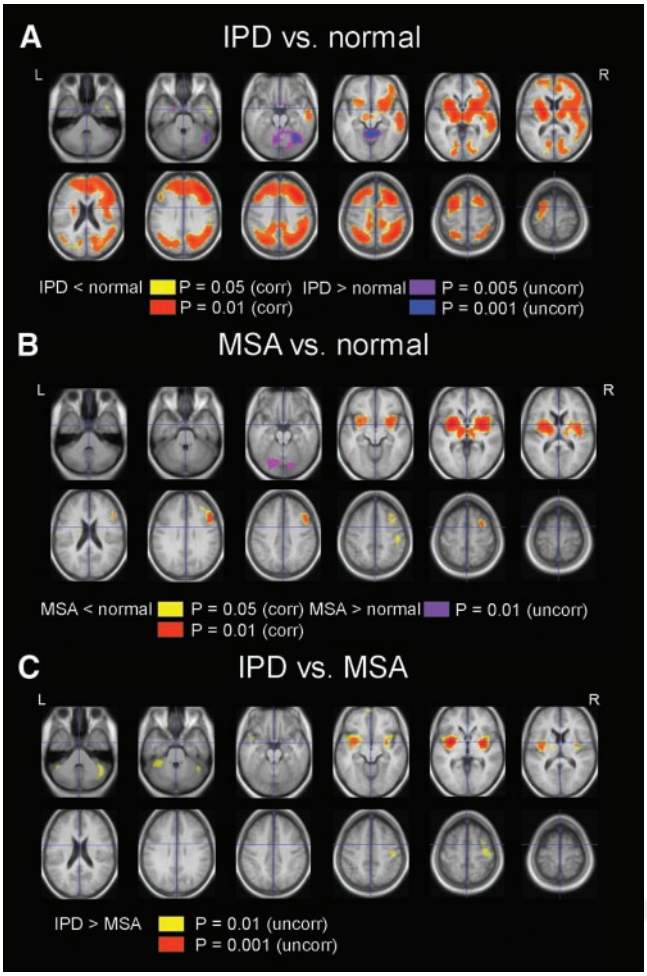

FIGURE 1. SPM maps of difference in ^{99m}Tc-ECD uptake between IPD patients, MSA patients, and healthy volunteers. Clusters are superimposed on a T1-weighted MR template constructed from healthy subjects in study. (A) IPD vs. healthy volunteers. (B) MSA vs. healthy volunteers. (C) MSA vs. IPD. Corr = corrected; uncorr = uncorrected.

tamen was found for MSA ($P = 0.001$, uncorrected), spreading laterally toward the amygdala and insula (especially on the left side). Additional infratentorial foci were present at the lateral cerebellar hemispheres but only at lower $P_{height} < 0.01$, uncorrected. These results are shown in Figure 1C and in Table 2. The intensity of the difference as determined by the contrast effect size at the posterior putamen (maximum voxel intensity at −33 0 0) is 16% (left) and 15.5% (right, 33 0 0). There were no regions where MSA patients showed more relative perfusion compared with IPD patients.

Cerebral Perfusion Correlates of Clinical Parameters

Disease Duration. In comparison with healthy subjects, the early disease group (lateralization flipped) showed a similar subcorticofrontal pattern but only with the absence of the posterior (parietooccipital) hypoperfusion (BA 39, 40) ($P < 0.01$, corrected) (Fig. 2A). Frontal hypoperfusion was predominant in the right-sided prefrontal and superior frontal cortex. The group with more advanced disease showed essentially the same pattern as the group as a whole (it has higher weight in the overall analysis with 61/81 patients), also with an added posterior cortical hypoperfusion (Fig. 2B).

Between both subgroups, significant differences were found in the anterior pons/substantia nigra and in both anterior medial temporal areas and posterior gyrus rectus (activity higher in the longer duration group) ($P_{height} < 0.001$, uncorrected) (Figs. 2C and 2D; Table 3). The group with longer disease duration showed less perfusion in the parietal association cortex and precuneus bilaterally (predominantly the right side, BA 7), as well as in the occipital cortex (BA 18, 19) (Fig. 2D). The same clusters were found for H&Y scores when the subgroup with H&Y I was compared with subgroup with H&Y II–IV.

No significant correlations with disease duration or H&Y score could be detected for MSA. When the MSA subgroup was compared with the early IPD group, similar differences were found with a relative hypoperfusion of the bilateral posterior putamen for MSA, albeit at a lower significance level ($P < 0.01$, uncorrected), likely due to the lower degrees of freedom (smaller IPD group).

Medication. There was no significant interaction between resting state perfusion and (chronic) levodopa medication level at the time of the scan. However, a significant correlation was found for IPD between increasing amounts of equivalent dopamine agonist and resting state perfusion, with a negative correlation between perfusion in both caudate heads and in the limbic system (left anterior and posterior cingulate, left fusiform gyrus, left parahippocampal gyrus) ($P_{height} < 0.001$, uncorrected) (Fig. 3; Table 4).

In the MSA group, the equivalent dopamine agonist level was inversely correlated with a more posterior reduction in resting perfusion in the pallidum/putamen ($P_{height} < 0.01$, uncorrected), but not in the caudate, as also shown in Figure 3 and Table 4. There was no correlation between clinical disease duration and dopamine agonist level.

Symptom Severity. Akinesia motor scores were inversely correlated with bilateral (left > right) and vermis cerebellar perfusion, only for the MSA subgroup (cluster level 0.003 corrected; voxel-level $P < 0.001$, uncorrected).

Common to both IPD and MSA, perfusion in the bilateral posterior associative cortex (inferior parietal lobule, precuneus) and posterior cingulate was negatively correlated with cognitive function ($P < 0.01$, uncorrected) (Fig. 4; Table 5). A positive correlation was found in mesolimbic and subcortical structures, but this did not reach significance at the cluster level.

The resting state perfusion could not be correlated with severity of the other motor parameters gait, postural instability, rigidity, and tremor or with autonomous signs in either patient group.

TABLE 2
SPM Results for Group Comparison (2-Sample t Test): IPD Patients vs. Healthy Subjects, MSA Patients vs. Healthy Subjects, and IPD Patients vs. MSA Patients

Cluster level	Voxel level		Coordinates				
P_{corr} (uncorr)	k_E	P_{corr} (uncorr)	t	*x*	*y*	*z*	Region (BA)
IPD patients vs. healthy subjects							
IPD patients < healthy subjects							
<0.001	5,229	<0.001	10	30	25	43	R middle frontal gyrus (BA 8)
		<0.001	9.59	15	−11	6	R thalamus (ventral lateral nucleus)
		<0.001	9.24	24	9	0	R lentiform nucleus, putamen + cluster also includes homonymous L-sided structures
<0.001	745	<0.001	9.38	−30	−62	47	L superior parietal lobule (BA 7)
		<0.001	7.31	−12	−47	47	L parietal lobe, precuneus (BA 7)
<0.001	1,495	<0.001	8.07	36	−53	47	R inferior parietal lobule (BA 40)
		<0.001	8.02	9	−33	43	R parietal lobe, precuneus (BA 7)
		<0.001	7.99	42	−47	47	R inferior parietal lobule (BA 40)
<0.001	166	<0.001	6.63	62	−29	−1	R middle temporal gyrus (BA 21)
IPD patients > healthy subjects							
0.005	805	0.04	4.52	9	−50	−8	Vermis
		0.14 (<0.001)	4.02	33	−62	−15	R upper cerebellar hemisphere
		0.16 (<0.001)	4.11	50	−59	−22	R upper cerebellar hemisphere
MSA patients vs. healthy subjects							
MSA patients < healthy subjects							
<0.001	2,098	<0.001	9.01	30	0	0	R lentiform nucleus, putamen
		<0.001	7.98	−33	0	3	L lentiform nucleus, putamen, claustrum
		<0.001	6.97	15	−14	6	R (+ L) thalamus, ventral lateral nucleus
<0.001	381	<0.001	6.22	50	22	29	R middle frontal gyrus (BA 9)
		<0.001	5.71	30	11	52	R middle frontal gyrus (BA 6)
		<0.001	5.17	33	20	46	R middle frontal gyrus (BA 8)
IPD patients vs. MSA patients							
MSA patients < IPD patients							
0.008	723	<0.001	5.79	33	−6	−2	R lentiform nucleus, putamen, claustrum
		0.01	4.93	39	8	−5	R insula (BA 13)
(0.042)	227	0.05	4.43	−33	0	0	L claustrum, lentiform nucleus, putamen

Corr = corrected; uncorr = uncorrected.

DISCUSSION

Differential Cerebral Perfusion Between MSA and IPD

In this study, rCBF patterns in IPD and MSA patients were investigated and compared with matched healthy individuals to show the topographic networks involved in the pathophysiology of both diseases. Comparison of IPD patients with healthy control subjects highlighted a decreased perfusion in an extensive mesencephalon-subcorticofrontal and parietotemporooccipital cortical topographic network. The data from this current cohort of patients with PD conform with ^{18}F-FDG PET studies with regard to the cortical pattern for advanced IPD (*15*,*16*).

The findings of bilateral subcortical hypoperfusion in the thalamus and lentiform nucleus with sparing of the caudate nucleus, irrespective of disease duration or severity, is at first sight at odds with ^{18}F-FDG PET data in the early course of the disease: generally, ^{18}F-FDG PET findings suggest that lentiform hypermetabolism in very early PD (<2 y) may be in part reversible (*17*,*18*). This has been explained by an increased tonic neuronal activity in the medial pallidum and subthalamic nucleus (*15*). Older study data have demonstrated no changes (*19*) or decreased perfusion in these areas for IPD (*20*). One possible explanation of why no upregulation in brain activity was found in this study is that, even for the short disease duration subgroup, most patients had their symptoms for >3 y. Second, levodopa may induce subcortical and, specifically, thalamic hypometabolism in early disease stages (*21*), although little is known on the chronic effects of levodopa on the perfusion pattern. Further studies with early and drug-naive IPD patients are needed to investigate the possible effect of striatal upregulation on perfusion.

The cortical perfusion differences found between healthy subjects and IPD patients in this study are in keeping with

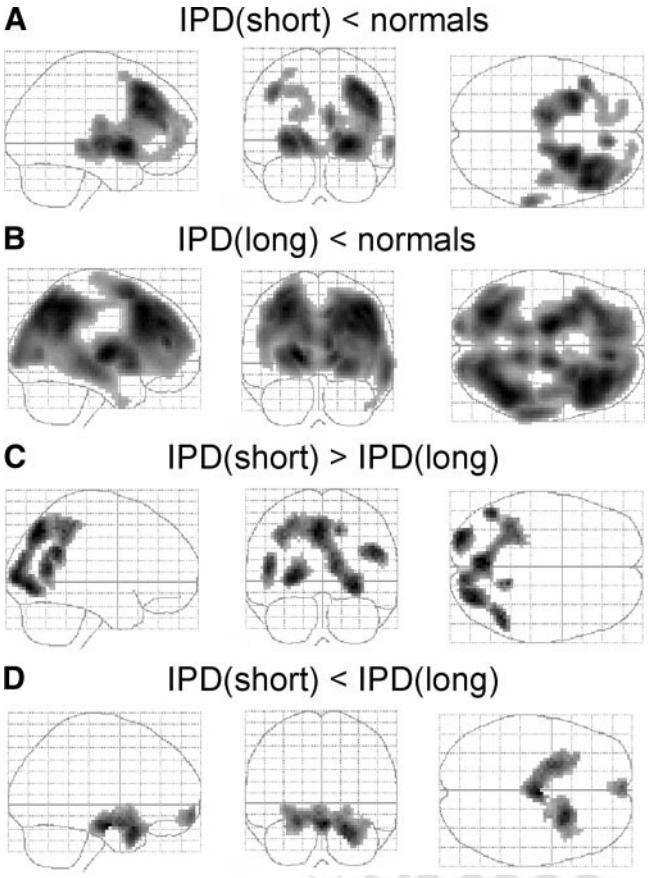

FIGURE 2. (A and B) SPM glass brain maps of difference in ^{99m}Tc-ECD uptake between IPD patients with disease of short (<5 y; A) and long (5–20 y; B) duration vs. healthy volunteers show contrast for decreased perfusion in patients. (C and D) SPM glass brain maps of difference in ^{99m}Tc-ECD uptake between IPD patients with disease of short (<5 y) and long (5–20 y) duration. (C) Contrast for relatively decreased perfusion in long-duration patients. (D) Contrast for relatively increased perfusion in long-duration patients.

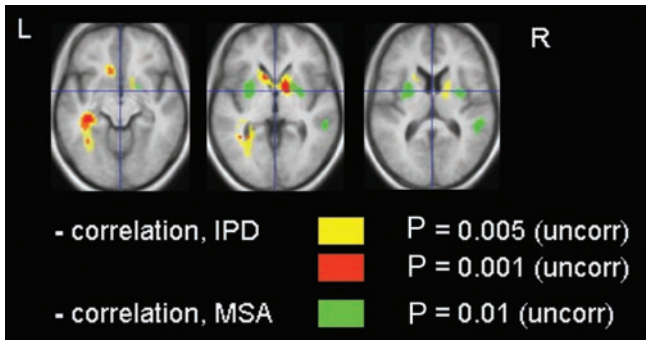

FIGURE 3. SPM maps of correlation analysis between regional ^{99m}Tc-ECD uptake in MSA and IPD patients vs. equivalent amount of dopamine agonist taken at time of SPECT study. Clusters are superimposed on T1-weighted MR template constructed from healthy subjects in study. Uncorr = uncorrected.

^{18}F-FDG PET (*22*,*23*) and perfusion SPECT (*24*) resting state studies, indicating widespread degeneration of normal cortical brain function, which, on progression of the disease, also involves posterior parietal association cortices.

As for MSA, it is well established that the dorsal putamen is the site first affected by MSA-S. In contrast to IPD, no associative cortical damage is seen, which may correspond to the relatively short disease duration, as MSA shows rapid disease progression. The hallmark information of posterior putamen hypoperfusion may be used for clinical discrimination, as the same differences are also present compared with the relatively early IPD group. Also, ^{18}F-FDG PET studies have demonstrated such differentiation between IPD and atypical parkinsonian syndromes (*23*,*25*). Whereas dopamine D_2 receptor-binding studies can aid significantly in differentiating between patients with good response to L-dopa and motor fluctuation development, functional imaging using indirect markers such as perfusion and metabolism may furthermore allow differentiation with other par-

TABLE 3
SPM Results for Group Comparison (2-Sample t Test) Between Short (<5 Years) and Long (5–20 Years) Disease Duration for IPD

Cluster level	Voxel level		Coordinates				
P_{corr} (uncorr)	k_E	P_{corr} (uncorr)	t	*x*	*y*	*z*	Region (BA)
Short disease duration > long disease duration							
<0.001	1,088	0.012	4.87	24	−84	4	R occipital gyrus (BA 19)
		0.012	4.87	18	−84	18	R cuneus (BA 18)
		(<0.001)	4.31	9	−59	50	R precuneus (BA 7)
0.001	466	(<0.001)	4.28	−24	−44	46	L precuneus (BA 7)
		(<0.001)	4.02	−45	−60	25	L middle temporal gyrus (BA 39)
Short disease duration < long disease duration							
0.013	985	(<0.001)	3.79	0	−13	−17	Brain stem, anterior
		(<0.001)	3.71	−24	8	−24	L superior temporal gyrus (BA 38)
		(<0.001)	3.64	24	17	−18	L inferior frontal gyrus (BA 47)

Corr = corrected; uncorr = uncorrected.

TABLE 4
SPM Results of Correlations Between Equivalent Dopamine Agonist Levels (DAL) Intake and Decreasing Perfusion for IPD and MSA

Cluster level	Voxel level		Coordinates				
$P_{corr\ (Small\ Volume\ Correction)}$	k_E	P_{corr} (uncorr)	t	*x*	*y*	*z*	Region (BA)
Perfusion inversely correlated with DAL for IPD							
0.015	107	0.043	4.53	−12	36	12	L anterior cingulate (BA 32)
	409	0.052	4.47	−39	−35	−6	L fusiform gyrus (BA 37)
		(0.001)	4.16	−33	−50	0	L parahippocampal gyrus (BA 19)
		(0.005)	2.63	−24	−58	14	L posterior cingulate (BA 31)
	478	(<0.001)	3.94	9	9	0	R caudate head
		(<0.001)	3.75	−12	23	−4	L caudate head
		(<0.001)	3.71	18	6	11	R lentiform nucleus, putamen
Perfusion inversely correlated with DAL for MSA							
0.03	150	(0.002)	2.88	27	0	3	R lentiform nucleus, putamen
		(0.008)	2.43	18	6	−5	R lentiform nucleus, putamen
	121	(0.004)	2.68	−27	3	5	L lentiform nucleus, putamen

Corr = corrected; uncorr = uncorrected.

kinsonian syndromes such as progressive supranuclear palsy (PSP) and other neurodegenerative diseases (*26*). These findings also underscore that frontal hypoperfusion is common in (moderate to advanced) IPD and, thus, that caution is mandatory if used to differentiate syndromes involving mainly frontal disturbances such as PSP (*27*). Although similar subcorticocortical degeneration mechanisms may play a role in the pathophysiology of MSA, this study shows that such cortical changes are not (yet) present in this group.

The relative hyperperfusion for IPD in the cerebellum and vermis conforms with earlier studies (*28*). In MSA, a relative hypometabolism in the cerebellum has been found (*29*,*30*), but this could not be demonstrated in this study of predominantly MSA-S patients.

Perfusion Correlates of Medication

Up till now, levodopa remains the most effective treatment for PD. Several groups have examined the effect of acute administration of L-dopa on rCBF and regional cerebral glucose metabolic rate in IPD patients and found either no differences in resting condition (*31*) or an inverse influence on pallidal blood flow (*32*,*33*); recent activation studies showed a decrease in the IPD-associated network activation and learning performance (*34*) and differential sensorimotor and prefrontal changes depending on chronic medication status. In our study, we were unable to confirm a significant interaction between resting perfusion and chronic levodopa medication level for IPD when compared with healthy subjects.

However, long-term effects of dopamine agonists on striatal perfusion were present. Chronic administration of dopamine agonists has been shown to result in downregulation of dopamine D_2 receptors, and, hence, decreased striatal synaptic activity may be expected (*35*). To our knowledge, this effect has not been demonstrated in vivo in patients with PD or MSA. The negative correlations found in our study could not be explained by disease duration acting as an underlying confounding factor as there was no correlation with dopamine agonist level. Although the current findings do not indicate whether

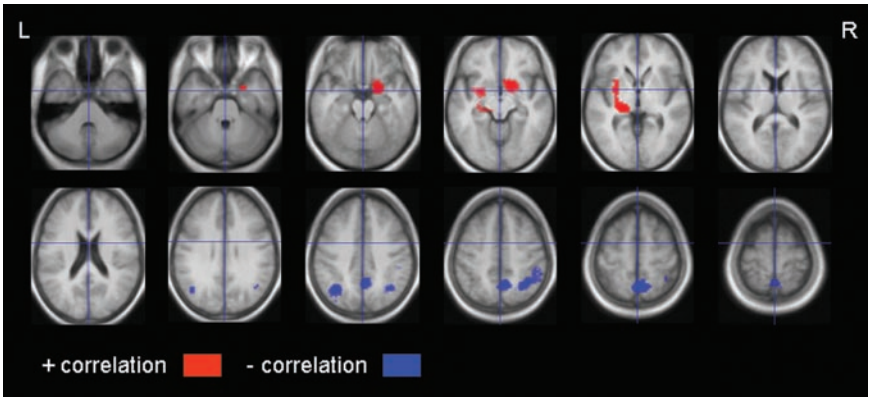

FIGURE 4. SPM maps of correlation analysis between regional ^{99m}Tc-ECD uptake in IPD patients vs. semiquantitative cognitive performance at time of SPECT study. Clusters are superimposed on T1-weighted MR template constructed from healthy subjects in study. − = negative correlation; + = positive correlation.

TABLE 5
SPM Results for Correlation Analysis Between Cognitive Performance and Perfusion in IPD and MSA

Cluster level	Voxel level		Coordinates				
P_{corr} (uncorr)	k_E	P_{corr} (uncorr)	t	*x*	*y*	*z*	Region (BA)
Perfusion inversely correlated with cognitive score for IPD							
(0.012)	1,858	(0.001)	3.14	9	−55	58	R precuneus (BA 7)
		(0.002)	3.04	6	−47	41	R cingulate gyrus (BA 31)
		(0.002)	2.97	33	−56	47	R inferior parietal lobule (BA 7)
	104	(0.012)	2.3	0	9	66	L superior frontal gyrus (BA 6)
(0.17)	467	(0.001)	3.15	−36	−59	42	L inferior parietal lobule (BA 7)
Perfusion inversely correlated with cognitive score for MSA							
0.06 (0.029)	155	(0.001)	4.09	3	−58	61	R precuneus (BA 7)
		(0.001)	4.03	−15	−52	69	L postcentral gyrus (BA 7)
		(0.001)	3.90	−6	−58	64	L precuneus (BA 7)
0.004	384	(0.001)	4.03	−39	−51	33	L inferior parietal lobule (BA 40)
		(0.001)	3.87	−59	−16	23	L postcentral gyrus (BA 3)

Corr = corrected; uncorr = uncorrected.

levodopa or dopamine agonists have a neuroprotective or neurotoxic effect on subcortical systems, the observation of differential indirect effects between IPD and MSA may direct investigations toward possible different action sites.

Perfusion Correlates of Clinical Parameters

For MSA, the symptom of akinesia in the MSA subgroup was specifically and inversely correlated with a large area in the cerebellar vermis and upper hemispheres, with a slight preference for the left-sided hemicerebellum, ipsilateral to the most dominant symptom hemisphere in this group. This suggests that cerebellar hypofunction may play a role in the control of movement in MSA and complies with the role of the area around the upper brain stem in the initiation and control of movement (*36*).

Previous resting state studies using ^{18}F-FDG PET in IPD have found increased thalamic activity correlated with tremor severity (*37*). In uncomplicated IPD, bradykinesia scores were found to be significantly positively correlated with the bilateral putamen and globus pallidum glucose metabolic rate, whereas tremor scores were negatively correlated with the bilateral putamen and cerebellar vermis cerebral metabolic rate of glucose (*38*), pointing to the major role of disruption of the striatofrontal and corticocerebellar pathways in the genesis of these extrapyramidal features. In this study, we were unable to find consistent relationships between motor scores and topographic networks in the brain for IPD, suggesting that various levels of regional activity may exist and pointing to the complexity of studying the underlying pathophysiology with a direct topographic analytic approach directed at functional localization.

Basal ganglia dysfunction has traditionally been associated with disturbances of movement. Nevertheless, in addition to motor dysfunction, cognitive abnormalities have been described in extension both in IPD as in MSA, but their underlying pathophysiology remains unclear. In our study, cognitive decline was associated with decreased perfusion in the parietal association cortex and in the occipital cortex and was positively correlated with mainly left limbic structures. The negative correlation findings are in accordance with ^{18}F-FDG PET results in IPD (*39*). Mentis et al. found specific correlation of these same regions with both visuospatial and mnemonic disturbances but not with dysphoria. Abnormalities at rest in regions subserving memory (mediotemporal) and visuospatial functioning (parietooccipital) regions confirm the possibility that cognitive dysfunction may be caused by a pathophysiologic process that affects the cortex globally rather than frontosubcortical regions locally. Previous theories have stated that executive function deficits reflect involvement of the dorsolateral prefrontal circuit as its projects through the basal ganglia and that basal ganglion dysfunction with disturbances of the anterior cingulate and orbitofrontal circuits are implicated as the anatomic substrate of behavioral alterations such as apathy, irritability, and dysinhibition, but this may be limited only to mood disorders and not necessarily to mnemonic and visuospatial (dys)function. Further prospective and correlation studies with more detailed neuropsychologic testing is needed to elucidate the underlying mechanisms involved in these areas.

Methodologic Issues

One drawback of this study is the inclusion of patients with a relatively long history of disease and in the course of drug treatment. Since differential diagnosis is an early problem, patients with disease duration of 1–2 y should also be studied.

From the methodologic point of view, the voxel-based approach has allowed accurate spatial localization of rCBF differences between groups such as localization in the mes-

encephalon and brain stem. Further improvement of anatomic localization may be possible by prior rigid coregistration of the functional SPECT data to the individual high-resolution MR images. As the results where localized in subcortical (sub)regions, this study also highlights the limitations of region-of-interest or volume-of-interest studies as these smooth out the precise anatomic–functional information in comparison with a data-driven whole-brain approach in SPM.

In this study only relative CBF values were used, which are susceptible to general arousal, aging, and drug effects. The global CBF of PD patients lowers with increasing disease duration and is lower by 15%–23% compared with that of healthy volunteers (*17*,*21*). In this work a global CBF analysis was not conducted; however, in view of the differences found, this still indicates that additional differential diagnostic information can be obtained using clinically available relative perfusion measurements. Levodopa and dopaminomimetics may differentially influence perfusion especially in the basal ganglia circuit. It is clear that additional study in the unmedicated state and comparative information with a larger study on short- and long-term effects of both levodopa and dopamine mimetics are needed to further clarify the (indirect) effect of these substances on regional metabolism and perfusion.

CONCLUSION

The rCBF pattern for PD corresponds to a fairly symmetric frontal–subcortical network involved in its pathophysiology, which is in accordance with the topographic organization suggested in the current model of basal ganglia–thalamocortical circuits. The typical feature of MSA-S is a localized bilateral posterior putamen hypoperfusion, which may lead further studies in very early parkinsonism for clinical discrimination. Differential effects of dopamine agonist medication were found between both disease entities, requiring more detailed study with respect to pathophysiology and possibly treatment response. Cognitive deterioration shows correlations with parietal association regions. This study also illustrates that voxel-based analysis of resting ^{99m}Tc-ECD SPECT holds considerable potential for assessing the neural substrates of chronic medication effects as well as clinical motor and cognitive impairment in PD.

REFERENCES

1. Hughes AJ, Daniel SE, Kilford L, Lees AJ. Accuracy of clinical diagnosis of idiopathic Parkinson's disease: a clinico-pathological study of 100 cases. *J Neurol Neurosurg Psychiatry.* 1992;55:181–184.
2. Antonini A, Moeller JR, Nakamura T, Spetsieris P, Dhawan V, Eidelberg D. The metabolic anatomy of tremor in Parkinson's disease. *Neurology.* 1998;51:803–810.
3. Henriksen L, Boas J. Regional cerebral blood flow in hemiparkinsonian patients: emission computerized tomography of inhaled ^{133}xenon before and after levodopa. *Acta Neurol Scand.* 1985;71:257–266.
4. Kuhl DE, Metter EJ, Riege WH. Patterns of local cerebral glucose utilization determined in Parkinson's disease by the [^{18}F]fluorodeoxyglucose method. *Ann Neurol.* 1984;15:419–424.
5. Wenning GK, Ben Shlomo Y, Magalhaes M, Daniel SE, Quinn NP. Clinical features and natural history of multiple system atrophy: an analysis of 100 cases. *Brain.* 1994;117:835–845.
6. Otsuka M, Ichiya Y, Kuwabara Y, et al. Glucose metabolism in the cortical and subcortical brain structures in multiple system atrophy and Parkinson's disease: a positron emission tomographic study. *J Neurol Sci.* 1996;144:77–83.
7. De Volder AG, Francart J, Laterre C, et al. Decreased glucose utilization in the striatum and frontal lobe in probable striatonigral degeneration. *Ann Neurol.* 1989;26:239–247.
8. Gilman S, Koeppe RA, Junck L, Kluin KJ, Lohman M, St Laurent RT. Patterns of cerebral glucose metabolism detected with positron emission tomography differ in multiple system atrophy and olivopontocerebellar atrophy. *Ann Neurol.* 1994;36:166–175.
9. Dethy S, Van Blercom N, Damhaut P, Wikler D, Hildebrand J, Goldman S. Asymmetry of basal ganglia glucose metabolism and dopa responsiveness in parkinsonism. *Mov Disord.* 1998;13:275–280.
10. Bosman T, Van Laere K, Santens P. Anatomically standardised ^{99m}Tc-ECD brain perfusion SPET allows accurate differentiation between healthy volunteers, multiple system atrophy and idiopathic Parkinson's disease. *Eur J Nucl Med Mol Imaging.* 2003;30:16–24.
11. Santens P, De Corte T, Vingerhoets G, Van Laere K, Dierckx R, De Reuck J. Regional cerebral blood flow and episodic memory in Parkinson's disease: a single photon emission tomography study. *Eur Neurol.* 2003;49:238–242.
12. Van Laere K, Versijpt J, Audenaert K, et al. ^{99m}Tc-ECD brain perfusion SPET: variability, asymmetry and effects of age and gender in healthy adults. *Eur J Nucl Med.* 2001;28:873–887.
13. Van Laere K, Koole M, Versijpt J, et al. Transfer of normal ^{99m}Tc-ECD brain SPET databases between different gamma cameras. *Eur J Nucl Med.* 2001;28:435–449.
14. Brett M, Christoff K, Cusack R, Lancaster J. Using the Talairach atlas with the MNI template [abstract]. *Neuroimage.* 2001;13:S85.
15. Eidelberg D, Moeller JR, Dhawan V, et al. The metabolic topography of parkinsonism. *J Cereb Blood Flow Metab.* 1994;14:783–801.
16. Hu MTM, Taylor-Robinson SD, Chaudhuri KR, et al. Cortical dysfunction in non-demented Parkinson's disease patients: a combined P-31-MRS and ^{18}FDG-PET study. *Brain.* 2000;123:340–352.
17. Imon Y, Matsuda H, Ogawa M, Kogure D, Sunohara N. SPECT image analysis using statistical parametric mapping in patients with Parkinson's disease. *J Nucl Med.* 1999;40:1583–1589.
18. Fukuda M, Edwards C, Eidelberg D. Functional brain networks in Parkinson's disease. *Parkinsonism Relat Disord.* 2001;8:91–94.
19. Sasaki M, Ichiya Y, Hosokawa S, et al. Regional cerebral glucose metabolism in patients with Parkinson's disease with or without dementia. *Ann Nucl Med.* 1992;6:241–246.
20. Markus HS, Costa DC, Lees AJ. HMPAO SPECT in Parkinson's disease before and after levodopa: correlation with dopaminergic responsiveness. *J Neurol Neurosurg Psychiatry.* 1994;57:180–185.
21. Ghaemi M, Raethjen J, Hilker R, et al. Monosymptomatic resting tremor and Parkinson's disease: a multitracer positron emission tomographic study. *Mov Disord.* 2002;17:782–788.
22. Eidelberg D, Edwards C. Functional brain imaging of movement disorders. *Neurol Res.* 2000;22:305–312.
23. Antonini A, Leenders KL, Vontobel P, et al. Complementary PET studies of striatal neuronal function in the differential diagnosis between multiple system atrophy and Parkinson's disease. *Brain.* 1997;120:2187–2195.
24. Kikuchi A, Takeda A, Kimpara T, et al. Hypoperfusion in the supplementary motor area, dorsolateral prefrontal cortex and insular cortex in Parkinson's disease. *J Neurol Sci.* 2001;193:29–36.
25. Otsuka M, Kuwabara Y, Ichiya Y, et al. Differentiating between multiple system atrophy and Parkinson's disease by positron emission tomography with ^{18}F-dopa and ^{18}F-FDG. *Ann Nucl Med.* 1997;11:251–257.
26. Eidelberg D, Takikawa S, Moeller JR, et al. Striatal hypometabolism distinguishes striatonigral degeneration from Parkinson's disease. *Ann Neurol.* 1993;33:518–527.
27. Okuda B, Tachibana H, Kawabata K, Takeda M, Sugita M. Cerebral blood flow in corticobasal degeneration and progressive supranuclear palsy. *Alzheimer Dis Assoc Disord.* 2000;14:46–52.
28. Owen AM, Doyon J, Dagher A, Sadikot A, Evans AC. Abnormal basal ganglia outflow in Parkinson's disease identified with PET: implications for higher cortical functions. *Brain.* 1998;121:949–965.
29. Taniwaki T, Nakagawa M, Yamada T, et al. Cerebral metabolic changes in early multiple system atrophy: a PET study. *J Neurol Sci.* 2002;200:79–84.

30. Gilman S. Biochemical changes in multiple system atrophy detected with positron emission tomography. *Parkinsonism Relat Disord.* 2001;7:253–256.
31. Leenders KL, Wolfson L, Gibbs JM, et al. The effects of L-DOPA on regional cerebral blood flow and oxygen metabolism in patients with Parkinson's disease. *Brain.* 1985;108:171–191.
32. Perlmutter JS, Raichle ME. Regional blood flow in hemiparkinsonism. *Neurology.* 1985;35:1127–1134.
33. Kobari M, Fukuuchi Y, Shinohara T, Obara K, Nogawa S. Levodopa-induced local cerebral blood flow changes in Parkinson's disease and related disorders. *J Neurol Sci.* 1995;128:212–218.
34. Carbon M, Ghilardi MF, Feigin A, et al. Learning networks in health and Parkinson's disease: reproducibility and treatment effects. *Hum Brain Mapp.* 2003;19:197–211.
35. Ekesbo A, Rydin E, Torstenson R, Sydow O, Laengstrom B, Tedroff J. Dopamine autoreceptor function is lost in advanced Parkinson's disease. *Neurology.* 1999; 52:120–125.
36. Nandi D, Aziz TZ, Liu X, Stein JF. Brainstem motor loops in the control of movement. *Mov Disord.* 2002;17(suppl 3):S22–S27.
37. Kassubek J, Juengling FD, Hellwig B, Knauff M, Spreer J, Lucking CH. Hypermetabolism in the ventrolateral thalamus in unilateral parkinsonian resting tremor: a positron emission tomography study. *Neurosci Lett.* 2001; 304:17–20.
38. Lozza C, Marie RM, Baron JC. The metabolic substrates of bradykinesia and tremor in uncomplicated Parkinson's disease. *Neuroimage.* 2002;17:688–699.
39. Mentis MJ, McIntosh AR, Perrine K, et al. Relationships among the metabolic patterns that correlate with mnemonic, visuospatial, and mood symptoms in Parkinson's disease. *Am J Psychiatry.* 2002;159:746–754.